Identification of molecular mechanisms underlying CIC-DUX4 tumor pathogenesis and aggressiveness

Introduction and study hypothesis

Undifferentiated round cell sarcomas (URCS) are aggressive soft tissue tumors that occur in children and young adults. Because of their morphological resemblance with Ewing sarcoma, they were referred as "Ewing sarcoma-like" tumors and are treated as canonical Ewing sarcomas despite their poor therapeutic response and aggressive clinical course (1). These tumors lack the canonical EWSR1-ETS fusion genes responsible for Ewing sarcoma pathogenesis and are instead relying on other genetic abnormalities such as, for the vast majority, the CIC-DUX4 translocation. The resulting aberrant fusion protein which is encoded by either the t(4;19)(q35;q13) or t(10;19)(q26;q13) chromosomal translocation, behaves as a transcription factor (TF), able to induce the expression of several target genes, including *ETV1, ETV4* and *ETV5*, which have been linked with sarcomagenesis (2). Due to their recent clinicopathological description (3), the molecular characterization of those tumors is still lacking and it is imperative to develop specific treatments for patients developing CIC-DUX4 sarcoma (CDS).

Hypothesis and aim of the study

Based on the current evidence showing the ability of CIC-DUX4 to induce a handful of target genes, we hypothesize that this fusion protein may function as an aberrant TF, modulating a critical network of genes responsible for sarcomagenesis, mainly through epigenetic remodeling mechanisms. More specifically, a report from 2016 showed that the endogenous DUX4 protein recruits p300 to its target genes to activate their transcription (4). Since CIC-DUX4 retains the DUX4 domain responsible for p300 recruitment we assume that the fusion protein relies at least to some extent on the same mechanism to establish its tumorigenic program. If this hypothesis is confirmed then p300 inhibition could represent an interesting therapeutic approach to treat CDS. To address these questions, we integrated epigenetic and transcriptional profiles of CIC-DUX4 tumor samples and tumor-derived cell lines, to identify the oncogenic pathways induced by the aberrant fusion protein. We are also taking advantage from our collaboration with Dr. T.Nakamura's group, who established an *ex-vivo* mouse model (Yoshimoto 2017) for CIC-DUX4 sarcoma, to develop new *in vivo* and in *vitro* models for further functional investigations.

Results

We used the ChIP-seq technology to characterize the epigenetic landscape of four primary CIC-DUX4 frozen tumors for key histone marks that define active promoters (H3K4me3) and enhancers (H3K4me1 and H3K27ac), as well as the repressive mark mediated by Polycomb Group Proteins (H3K27me3). Figure 1 shows examples of actively expressed genes in three primary tumors from which we obtained the complete histone marks characterization. The epigenetic profiling of these tumors has been analyzed and paired with the RNA-seq data obtained from the same samples by Prof. Antonescu's lab, at the MSKCC in New York. This first analysis provided us a set of critical information about the ability of CIC-DUX4 to establish its tumorigenic program in primary human tumors, and constitute a reference model for any comparative analysis performed in tumor-derived cell lines.

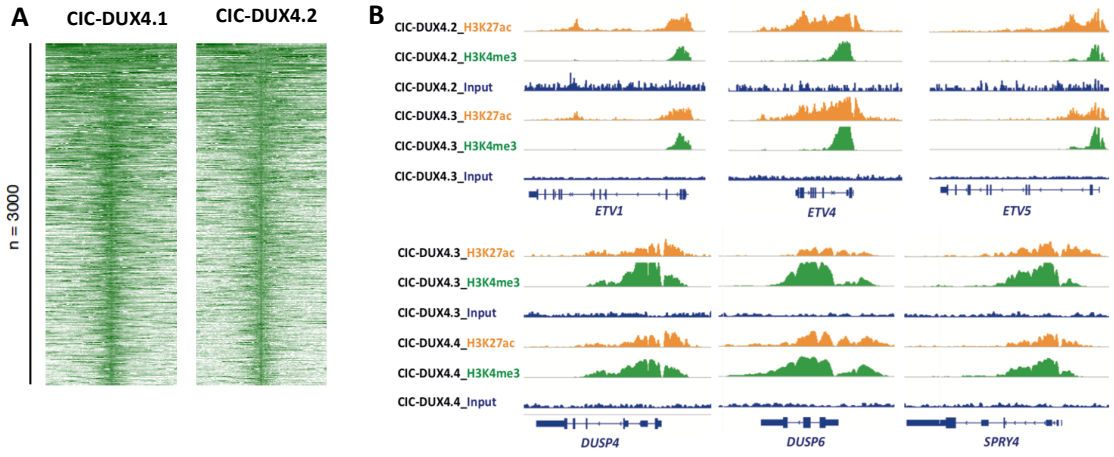

Fig. 1 CIC-DUX4 primary tumors' chromatin profile
A. Heatmap of the 3000 highest H3K27ac signal intensities shared by two primary CIC-DUX4 tumors. **B.** ChIP-seq tracks of three primary CIC-DUX4 tumors showing H3K27ac and H3K4me3 enrichment at specific CIC-DUX4 target sites.

In parallel we also expanded one primary CIC-DUX4 cancer cell line (CDS1) and one PDX (patient derived xenograft)-derived CIC-DUX4 cancer cell line (CDS2). After characterizing these two cell lines for CIC-DUX4 expression at mRNA and protein levels, we confirmed their tumorigenicity by injecting them subcutaneously in immunocompromised mice. H&E staining of the tumor xenografts revealed a small blue round cell phenotype (**Figure 2A**) recapitulating the morphology of the parental tumor. In agreement with a report

showing that DUX4 immunohistochemistry is a highly sensitive and specific diagnostic tool for CIC-DUX4 sarcoma (5), we performed DUX4 IHC on our cell lines derived tumors and noticed an overall nuclear positivity for DUX4 staining but also some regions of low or absent nuclear signal, an histological pattern not reported in any previous work (**Figure 2B**). The reason for this heterogeneity is currently under investigation.

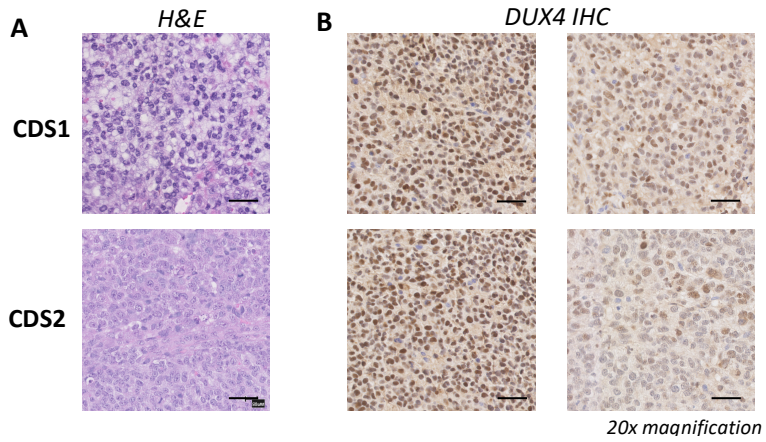

Fig. 2 H&E and DUX4 immunohistochemistry of CDS1 and CDS2 derived tumors.
A. H&E staining of CDS1 and CDS2 derived tumors. **B.** DUX4 IHC from the same CDS1 and CDS2 derived tumors. High nuclear DUX4 signal (left) and low nuclear DUX4 signal (right) are both shown from the same tumor.

Next, we performed ChIP-seq on the CDS1 and CDS2 cell lines for the same histone marks profiled in the CDS primary tumors and surveyed the CIC-DUX4 and p300binding sites. Since the two cell lines don't express the endogenous DUX4, we could use an anti-DUX4 antibody to specifically identify the binding profile and direct target genes of the translocation in both models.

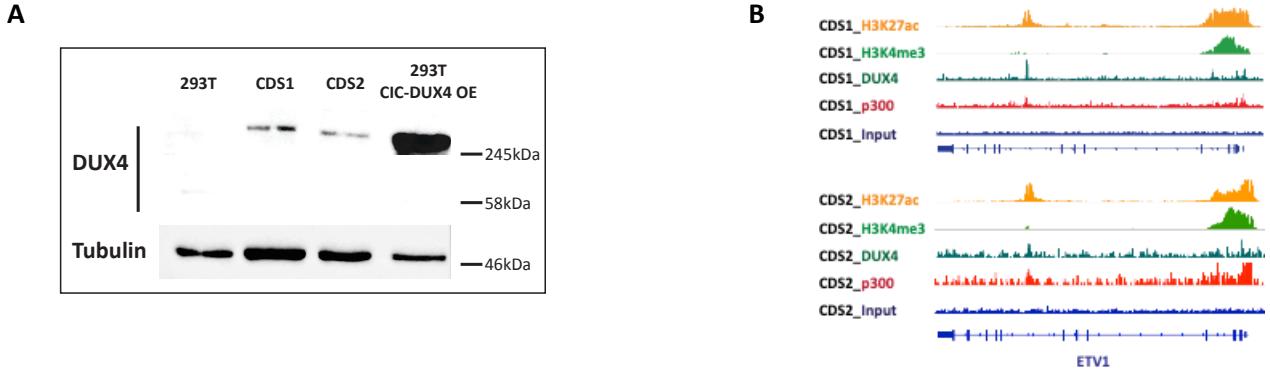

Fig. 3 CDS1 and CDS2 characterization and ChIP-seq profile.
A. Western Blot analysis for CIC-DUX4 expression in CDS1 and CDS2 compared to wild type 293T cells, as well as 293T cells in which CIC-DUX4 is overexpressed (293T CIC-DUX4 OE). **B.** ChIP-seq tracks for CDS1 and CDS2 cell lines.

We also performed an immunofluorescence (IF) assay for DUX4 in our two cell lines to evaluate the intensity, distribution and subcellular localization of CIC-DUX4 (**Figure 4**). Surprisingly, the IF signal for DUX4, although present in the nuclei of both CDS1 and CDS2 cells, also appeared to be located at the perinuclear membrane and in the cytoplasm, suggesting that this fusion portein may shuttle from the nucleus to the cytoplasm, as recently reported for the wild type CIC protein, and potentially display additional non-nuclear functional properties.

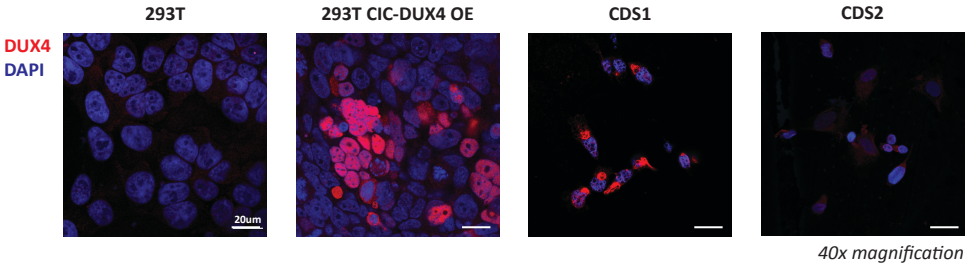

Fig. 4 DUX4 immunofluorescence in CDS1 and CDS2 cell line
Immunofluorescence analysis using an anti-DUX4 antibody (red) and DAPI (blue). 293T, 293T-CIC-DUX4 OE, CDS1 and CDS2 cells were compared for their CIC-DUX4 expression patterns.

Following this observation, we surveyed the currently available literature for any known mechanism of CIC-DUX4 nucleo-cytoplasmic shuttling or degradation regulation, but only found such a mechanism for the wild type CIC protein. In several studies, CIC has been shown to shuttle from the nucleus to the cytoplasm, where it is degraded by the ubiquitin proteasome pathway upon MAPK activation.

Since the CIC protein is almost completely preserved in the CIC-DUX4 fusion, we investigated whether CIC-DUX4 protein stability was also dependent on MAPK activation status by testing different culture conditions. To this end, we grew CDS1 and CDS2 cells either in standard culture medium (containing 10% FBS as in our previous experiments), or in media containing either 10%, 5%, 3% or 1.5% FBS. To evaluate further the effect of growth factors on CIC-DUX4 localization, stability and expression, we also grew the CDS1 and 2 cell lines in culture medium containing KO replacement serum with or without Epidermal Growth Factor (EGF, a powerful activator of the MAPK pathway), and performed IF and WB analysis after 3, 5 and 7 days of culture in the different media formulations. Although we didn't observe any striking cellular morphological differences between the tested conditions (data not shown), Western Blot signals for CIC-DUX4 were decreasing in the later timepoints compared to the first ones, suggesting a possible role of cell adhesion in the stability of CIC-DUX4 protein. Thus, we hypothesized that CIC-DUX4 protein levels may progressively decrease as the cells adhere to the plastic surface of the culture dishes. We also performed a ChIP-seq analysis for DUX4 in CDS2 cell line after cultivating them in adherent or low adherent conditions in different serum conditions (**Figure 5**).

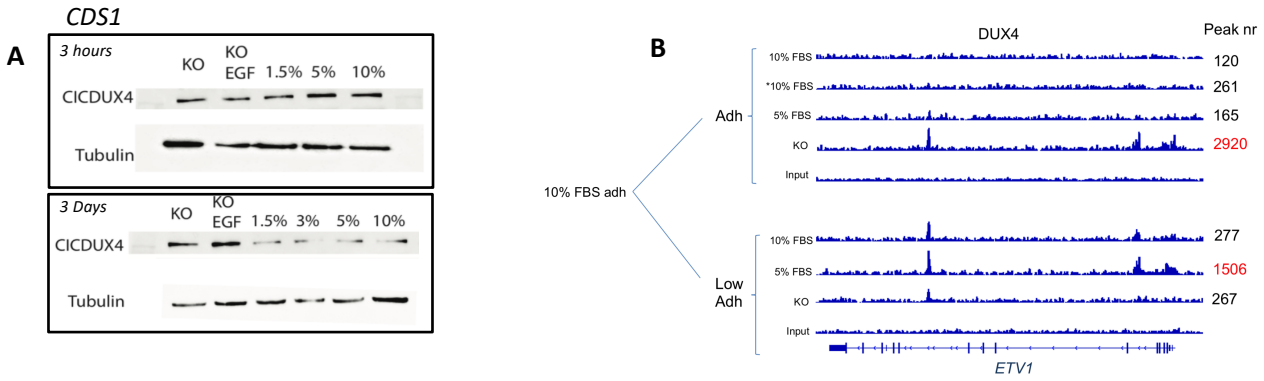

Fig. 5 Effect of different culture conditions on CDS1 and CDS2 cell lines and CIC-DUX4 expression.
A. Western Blot of CIC-DUX4 in CDS1 cultured in adherent condition with media containing different FBS concentrations (1.5%, 5% and 10%), KO serum and KO + EGF after 3 hours and 3 days. **B.** ChIP-seq analysis for DUX4 of CDS2 in adherent versus low-adherent culture conditions with varying serum concentrations. Cells from every condition were harvested 7 days after plating except for *10%FBS condition which was harvested 1 day after plating. DUX4 peaks number > 1000 are shown in red.

As shown in **Figure 5**, CIC-DUX4 binding frequency varies dramatically among the different culture conditions. Since the CIC-DUX4 DNA binding frequency appears to be enhanced in KO serum in adherent culture conditions, we decided to perform all further experiments in these conditions, and are currently analyzing the CDS1 and CDS2 ChIP-seq profiled obtained in the new KO culture conditions.

To validate the importance of CIC-DUX4 on the expression of its known target genes in our CDS1 and CDS2 cellular models we then performed a knockdown of the fusion protein in these cells using two shRNAs (shDUX4 33 and shDUX4 34) targeting the 3' end of the DUX4 transcript. As shown in **Figure 6**, both shRNAs induced a decrease in the mRNA levels for CIC-DUX4 and its target genes mRNA in 10% FBS-containing medium. To be able to compare this experiment with the data obtained from the wild type CDS1 and CDS2 characterization, we are currently performing the same knockdown experiment in both cell lines grown in KO condition. The CIC-DUX4 knockdown will allow us to investigate how the removal of CIC-DUX4 fusion changes the global epigenetic landscape and gene expression profile of our cell lines in order to define new CIC-DUX4 targets and investigate their potential therapeutic implication in CIC-DUX4 sarcoma treatment.

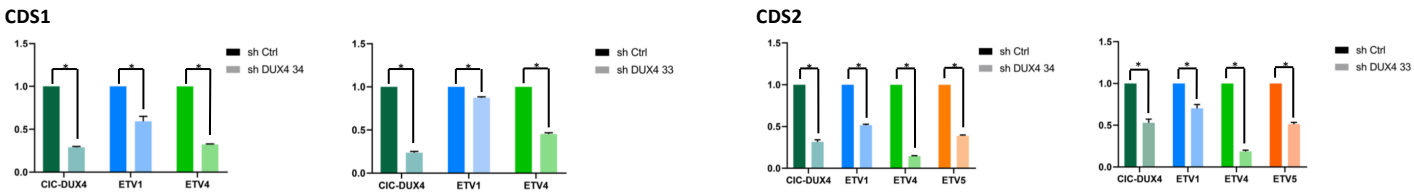

Fig. 6 Characterization of CIC-DUX4 and its target genes' mRNA after DUX4 knockdown in CDS1 and CDS2
Data are presented as mean +/- SD, with n=3 per group. Unpaired, independent groups of 2 were analyzed by Student's t test.
*P < 0.05.

Next, in order to investigate the function of the CIC-DUX4 protein during the first steps of tumor formation, we generated a cellular model where CIC-DUX4 was expressed exogenously. To this end, we took advantage of a "Tet-on" inducible system using a plasmid containing a Flag tagged CIC-DUX4 sequence. For our initial experiment we used human pediatric mesenchymal stem cells (hpMSCs),

since these cells has been reported to recapitulate the cell of origin for a subset of sarcomas, and infected them with lentiviral particles containing the CIC-DUX4 plasmid or an empty vector. We observed an induction of CIC-DUX4 expression at the mRNA and protein level, as well as an induction of CIC-DUX4 target genes' mRNA after doxycycline treatment (**Figure 7A and B**, left). However, when we compared ChIP-seq tracks of CIC-DUX4 expressing hpMSCs and control hpMSCs we didn't observe any significant change and couldn't find any signal for CIC-DUX4 binding in both conditions (**Figure 7C,** left). We then performed IF on CIC-DUX4 expressing hpMSCs and found out that only a small fraction of all cells was expressing the fusion protein (**Figure 7d,** left), suggesting that this cellular model is not permissive for the expression and function of the CIC-DUX4 fusion protein.

To circumvent the biological limitations inherent to the hpMSCs model, we then performed the same infection experiment using the 293T cell model, a well-established cell line known to tolerate the expression of several oncogenes. CIC-DUX4 protein expression was induced and CIC-DUX4 target genes transcripts were more expressed in CIC-DUX4 infected cells compared to control (**Fig. 7A-B**, right). Accordingly, 293T cells showed a strong increase in the H3K27ac histone mark at specific genomic loci bound by CIC-DUX4 in the CDS1 cell line (**Fig. 7C**, right). The ChIP-seq for DUX4, FLAG and p300 are currently being sequenced. We also performed DUX4 IF on 293T cells expressing CIC-DUX4 and identified a higher fraction of 293T cells showing strong DUX4 nuclear positive signal compared to hpMSCs (**Fig. 7D**, right). Even if in 293T where CIC-DUX4 is overexpressed (C-D OE) this represent only a fraction of all infected cells, it was sufficient to observe global epigenetic changes using ChIP-seq. Based on these results, we showed that different cell types harbor variable permissiveness to CIC-DUX4 expression and that CIC-DUX4 induction is sufficient to reprogram the epigenome of cells and establish a specific CDS epigenetic signature.

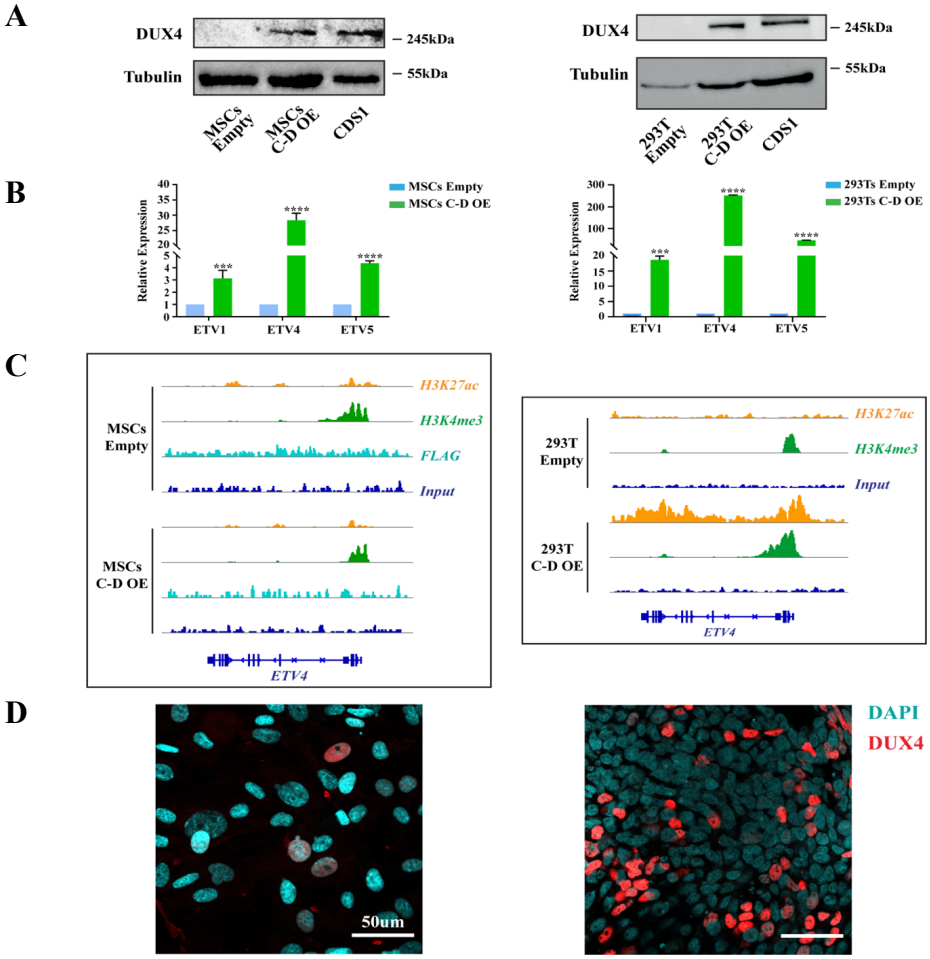

Fig. 7 CIC-DUX4 induction in hpMSCs and 293T cells.

A. Western Blot showing the expression of the CIC-DUX4 protein in induced hpMSCs (left) or 293T (right) compared to CDS1 cell line. **B.** qPCR showing the induction of PEA3 genes expression in control cells infected with an empty vector compared to cells infected with CIC-DUX4 containing vector. Left panels illustrate hpMSCs whileand right panels show 293T experiments.
Data are presented as mean +/- SD, with n=3 per group. Unpaired, independent groups of 2 were analyzed by Student's t test. *P = 0.01 to 0.05, **P = 0.001 to 0.01, ***P = 0.0001 to 0.01, ****P<0.0001. **C.** ChIP-seq for H3K27ac, H3K4me3 and Flag showing no differences between control hpMSCs and CIC-DUX4 expressing hpMSCs (left). ChIP-seq for H3K27ac and H3K4me3 showing the induction of the H3K27ac histone mark at ETV4 promoter in 293T expressing CIC-DUX4 cells. **D.** Immunofluorescence for CIC-DUX4 on either hpMSCs C-D OE (left) or 293T C-D OE (right).

Finally, we hypothesize that CIC-DUX4, which contains the required DUX4 amino acids to induce p300 recruitment (4), activates its target genes' transcription through the same mechanism. If this is true, p300 pharmacological inhibition may represent an interesting therapeutic approach for CIC-DUX4 sarcoma treatment. We took advantage of the recent discovery of A-485, a specific inhibitor of p300 catalytic activity, to test p300 inhibition in our two CIC-DUX4 sarcoma cell lines. We followed the same treatment protocol published in the original report and integrated our results in the screening of cancer cell lines for p300 inhibition sensitivity reported in the same study (4). Interestingly, CDS1 and CDS2 cell lines were among the top 10 most sensitive cell lines toward p300 inhibition after 5 days of treatment (**Figure 8**). Moreover, p300 pharmacological inhibition and shRNA against p300 induced a decrease in CIC-

DUX4 target genes' expression without impairing CIC-DUX4 transcription itself. Intriguingly, after 5 days of treatment with A-485, the expression of the CIC-DUX4 protein itself was found to be strongly reduced in both cell lines with increasing concentration of the inhibitor. We are currently investigating the mechanism by which p300 inhibition lowers CIC-DUX4 protein levels since this feature may have significant clinical implications.

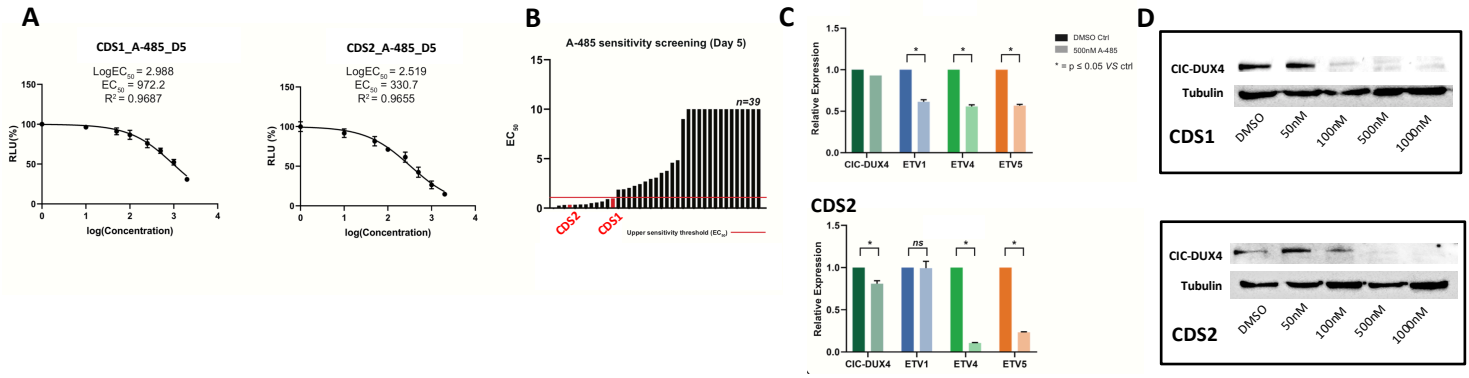

Fig. 8 p300 inhibition in the CDS1 and CDS2 cell lines
A. EC50 calculation for CDS1 and CDS2 cells treated with the p300 inhibitor A-485. GraphPad Prism non-linear regression model was used to generate the dose-response curve and to obtain the EC50 value. **B.** Comparison of CDS1 and CDS2 in vitro EC50 for A-485 to the original cell screening results. **C.** CIC-DUX4 and target genes' mRNA expression in CDS1 and CDS2 cell lines after A-485 treatment. Data are presented as mean +/- SD, with n=3 per group. Unpaired, independent groups of 2 were analyzed by Student's t test. *P < 0.05. **D.** CIC-DUX4 protein expression in CDS1 and CDS2 after A-485 treatment with increasing concentration.

In order to validate the results obtained in vitro we injected subcutaneously 2 million CDS2 cells bilaterally in the suprascapular region of 10 NOD-SCID gamma KO mice. 4 weeks later, once small tumors developed at all injection sites, we started intraperitoneal A-485 injections twice daily. 5 mice received 100mg/kg A-485 based on their weight at the first day of injection and 5 mice received the corresponding volume of carrier without A-485. Based on available in vivo studies using A-485, our initial plan was to continue the same treatment regimen for 15 days, and generate a survival curve. Unfortunately, we had to stop the experiment after 12 days due to a 10-20% weight loss of the mice receiving the A-485 treatment. As a consequence, control and treated mice were sacrificed sequentially during 4 days as shown on the timeline of **Figure 9A**. However, despite the early interruption of the treatment, we observed a strong reduction in both tumor volume and size compared to control mice (**Fig. 9B**). Given this promising preliminary result, the experiment will be replicated using 50mg/kg A-485 as initial dose, and adapting it to the weight of each mice throughout the treatment in order to reduce side effects.

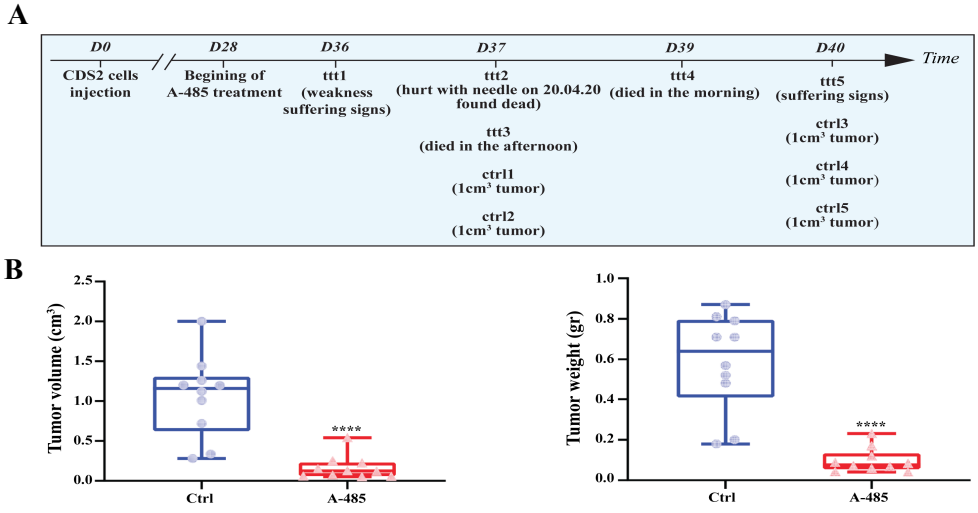

Fig. 9 In vivo A-485 treatment of CDS2-derived tumors.
A. Timeline showing the date of mice sacrifices. Ttt = treated mouse. Ctrl = control mouse. () = reason of sacrifice
B. Left panel: tumor volume in cm3 for each tumor collected at the day of sacrifice. Right panel: tumor weight for each tumor collected at the day of sacrifice. Difference between tumor volumes and weights were analyzed by Mann-Whitney U test. *P = 0.01 to 0.05, **P = 0.001 to 0.01, ***P = 0.0001 to 0.01, ****P<0.0001

To summarize, in this study we describe for the first time the genome wide epigenetic profile of primary CDS tumors and derived cells lines, including the direct binding sites of the CIC-DUX4 fusion protein. This information will be combined with available gene expression profiles to generate a comprehensive set of direct target genes of the fusion protein. We will then implement these results with both knock-down and expression studies in CDS lines and 293T cells, respectively, to refine the target repertoire and identify the most important and responsive genes. Finally, the identification of p300 as a critical molecular player in CDS biology may provide a new promising target for the clinical management of these aggressive tumors.

References

1. Machado I, Navarro S, Llombart-Bosch A. Ewing sarcoma and the new emerging Ewing-like sarcomas: (CIC and BCOR-rearranged-sarcomas). A systematic review. Histol Histopathol [Internet]. 2016 Nov [cited 2017 Aug 21];31(11):1169–81. Available from: http://www.ncbi.nlm.nih.gov/pubmed/27306060
2. Kawamura-Saito M, Yamazaki Y, Kaneko K, Kawaguchi N, Kanda H, Mukai H, et al. Fusion between CIC and DUX4 up-regulates PEA3 family genes in Ewing-like sarcomas with t(4;19)(q35;q13) translocation. Hum Mol Genet [Internet]. 2006 [cited 2017 Aug 21];15(13):2125–37. Available from: https://oup.silverchair-cdn.com/oup/backfile/Content_public/Journal/hmg/15/13/10.1093/hmg/ddl136/2/ddl136.pdf?Expires=1503421251&Signature=JZpB9Bzy7K35DhFngRHqP3KXyA8IrBZTJIPDo6uBACHM9v9q4JL09jNhr6x9E7SEnlH-KiSqilx~k7KP6lhCP63EG-XEUz32gE2CBoS2nNjI3bULuldg
3. Specht K, Sung Y-S, Zhang L, S Richter GH, Fletcher CD, Antonescu CR. Distinct Transcriptional Signature and Immunoprofile of CIC- DUX4–Fusion Positive Round Cell Tumors Compared to EWSR1- Rearranged Ewing Sarcomas – Further Evidence Toward Distinct Pathologic Entities. Genes Chromosom Cancer [Internet]. 2014 [cited 2017 Aug 21];53(7):622–33. Available from: https://www.ncbi.nlm.nih.gov/pmc/articles/PMC4108073/pdf/nihms612380.pdf
4. Choi SH, Gearhart MD, Cui Z, Bosnakovski D, Kim M, Schennum N, et al. DUX4 recruits p300/CBP through its C-terminus and induces global H3K27 acetylation changes. Nucleic Acids Res [Internet]. 2016 Jun 20 [cited 2018 Nov 20];44(11):5161–73. Available from: https://academic.oup.com/nar/article-lookup/doi/10.1093/nar/gkw141
5. Siegele B, Roberts J, Black JO, Rudzinski E, Vargas SO, Galambos C. DUX4 Immunohistochemistry Is a Highly Sensitive and Specific Marker for CIC-DUX4 Fusion-positive Round Cell Tumor [Internet]. 2016 [cited 2018 Dec 4]. Available from: www.ajsp.com.